Relaxation of residual stresses induced by laser shock processing

C. Rubio-González
Centro de Ingeniería y Desarrollo Industrial,
Pie de la cuesta No. 702, Desarrollo San Pablo, Querétaro, Qro., 76130, México,
Tel: +52(442)2119838, fax: +52(442)2119839,
e-mail: crubio@cidesi.mx

A. Garnica-Guzmán
Instituto Tecnológico de Morelia,
Av. Tecnológico 1500, Morelia, Mich. 58120, México.

G. Gómez-Rosas
Departamento de Física, Centro Universitario de Ciencias Exactas e Ingenierías, CUCEI.
Universidad de Guadalajara, Blvd. Marcelino García Barragán 1421,
Guadalajara Jalisco, 44430, México.

Recibido el 27 de mayo de 2008; aceptado el 20 de abril de 2009

The Laser shock processing (LSP) is a new surface treatment technique that induces a compressive residual stress field. This work examines the effect of cyclic loading and temperature on the stability of the stress field induced by LSP on 6061-T6 aluminum samples. Residual stress relaxation due to cyclic loading is reported for different stress amplitudes and temperatures. Due to the cyclic creep effect, the residual stress decreases linearly with the logarithm of the number of cycles, N.

Keywords: Laser shock processing; residual stress relaxation; cyclic loading.

El Proceso de Impacto con Láser (LSP) es una técnica novedosa para el tratamiento de superficies que induce campos de esfuerzos residuales de compresión. Este trabajo examina los efectos de cargas cíclicas y el efecto de la temperatura en la estabilidad de los campos de esfuerzos inducidos por la técnica LSP en muestras de aluminio 6061-T6. Se reporta la relajación de esfuerzos residuales debidos a las cargas cíclicas para diferentes amplitudes de esfuerzos y diferentes temperaturas. Debido a los efectos de la fluencia cíclica, los esfuerzos residuales decrecen linealmente con el logaritmo del número de ciclos, N.

Descriptores: Proceso de impacto láser; relajación de esfuerzos residuales; cargas cíclicas.

PACS: 42.62.-b; 42.62.Cf; 81.40.Lm

1. Introduction

Laser Shock Processing (LSP) is a new and promising surface treatment technique that has been shown to be effective in improving the fatigue and fracture properties [1] and wear resistance [2] of a number of metals and alloys. Potential applications are directed to aerospace and automotive industries. The beneficial effects of LSP on static, cyclic, fretting fatigue and stress corrosion performance of aluminum alloys, steels and nickel-based alloys have been demonstrated [3-9]. Since laser beams can be easily directed to fatigue-critical areas without masking, LSP technology is expected to be widely applicable for improving the fatigue properties of metals and alloys, particularly those that show a positive response to shot peening.

The stability of the mechanically treated surface of components during the application of thermal and/or mechanical energy is desirable to preserve improvements in the mechanical properties. In this connection, residual stress relaxation behavior is the most important aspect to consider. Macro and micro residual stresses can be reduced or completely relaxed either by heat treatment or under unidirectional or cyclic mechanical loading [10].

Cyclic loading may relax the residual stress field decreasing the beneficial effect of the LSP. In addition high temperatures may accelerate the relaxation process. If it is desirable to use LSP in industrial applications, it is necessary to have a deep knowledge and understanding of the process and to evaluate the effect of temperature and cyclic loading on the stability of the residual stress field.

A report of thermal relaxation, quasistatic and cyclic relaxation of shot peening induced residual stresses is presented in Ref. 11 for AISI 4140 steel. There are results reported in the open literature about relaxation of residual stresses induced by shot peening in different materials [10,12]. Few results are reported, however, for relaxation of LSP induced residual stresses [12,13]. As shown in Ref. 12, the effect of shot peening and LSP may be different, for example, the degree of cold work at the surface can be exceptionally high for shot peening (up to 30% - 40%) while it is beneficially less (9% or less) for LSP.

The objective of this work is to analyze the stability of residual stress field induced by LSP on 6061-T6 aluminum alloy samples during the application of cyclic loading and thermal energy.

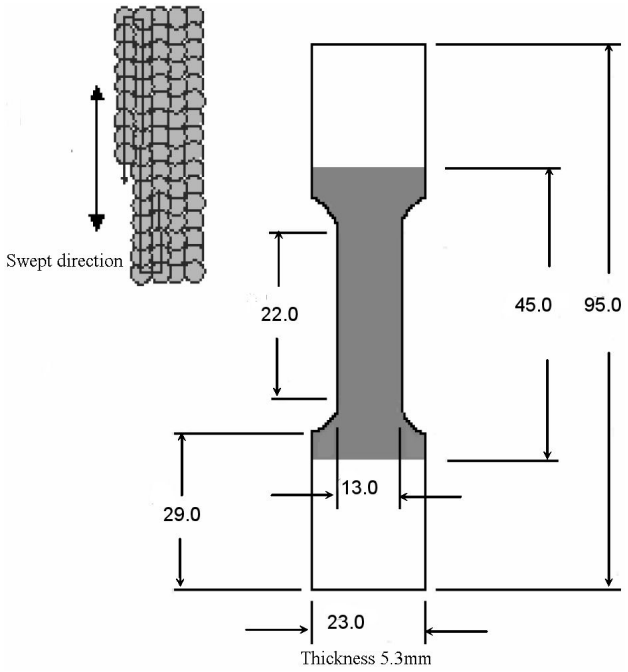

FIGURE 1. Specimen geometry and LSP swept. Dimensions in mm.

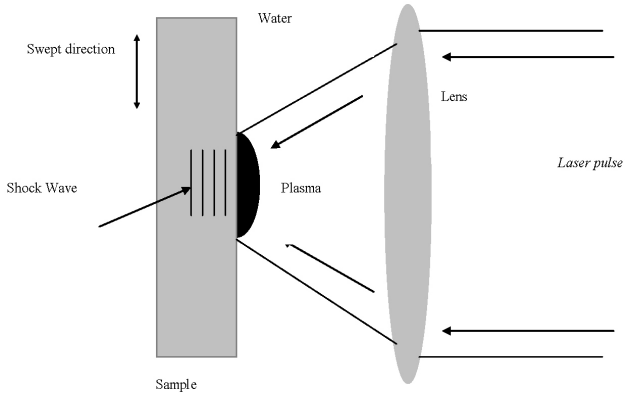

FIGURE 2. Principle of Laser Shock Processing.

Residual stress relaxation occurs when a critical value of the applied loading stress amplitude is exceeded and a cyclic direct dislocation movement converts the elastic strain associated with the macro residual stress into micro plastic strain [11]. Alterations of the shot peening induced residual stresses at the surface with the number of cycles have been observed [10]. This behavior may be described by a linear dependence of the residual stress on the logarithm of the number of cycles, N, according to a logarithm creep law:

$$\sigma = A - m \log N \tag{1}$$

due to the so-called cyclic creep, where the properties A and m can be determined for each stress amplitude and thermal condition from the experimental data in the linear sections of the curves.

2. Experimental work

The methodology used in the experimental work is presented next. First the specimen material and geometry are described. Then the procedures used in the residual stress measurements and the relaxation tests are explained.

Material

Commercial laminated plates of aluminium 6061-T6 and 6.3 mm thick were machined to get the specimens with thickness 5.3 mm. Specimens were then treated with LSP. The T6 condition consists of a solution treatment and natural aging. Its chemical composition (wt%) was: 0.52 Si, 0.27 Fe, 0.13 Cu, 0.03 Mn, 0.46 Mg, 0.011 Zn, 0.27 Cr, 0.022 Ti. This composition was determined using a spark emission spectrometer [1,14]. The mechanical properties were determined using dog-bone type specimens [1]. The offset tensile yield stress is 226 MPa, ultimate tensile strength 250 MPa and elastic modulus 59.7 GPa. Figure 1 shows the specimen dimensions, the treated area and the swept direction. The swept direction is parallel to the specimen longitudinal axis. Both specimen faces were treated with the same swept direction.

Laser shock processing

The LSP experiments were performed using a Q switched Nd:YAG laser operating at 10 Hz with a wave length of 1064 nm and the FWHM of the pulses was 8 ns. A convergent lens is used to deliver 2.5 J, see Fig. 2. Spot diameter was 1.5 mm. Only one pulse density was used: 5000 pulses/cm^2. Specimens were submerged into a water bath, where water was the confined medium, while they were irradiated. A 2D motion system was used to control the specimen position and to generate the pulse swept as shown in Fig. 2. Controlling the velocity of the system, led to the desired pulse density.

Usually the residual stress profile obtained by LSP and shot peening has tensile stresses near the surface (on short depths) and compressive stresses inside the material. Before the LSP treatment, the specimen surface was painted by hand using commercial non-bright black paint. This process was performed carefully to obtain a uniform paint layer with thickness of about 13 μm. The advantages of placing an absorbent overlay on the sample surface before LSP treatment has been demonstrated in Ref. 15. Painting the sample surface makes the compressive stress profile move to the surface, that is, the maximum compressive stress is reached sooner in all the specimen depths.

Once the specimens were LSP treated, a thin surface layer was eliminated carefully grinding the surface. The purpose of grinding was to eliminate the rough surface (see Fig. 3) and to avoid errors during residual stress measurements by X-ray diffraction.

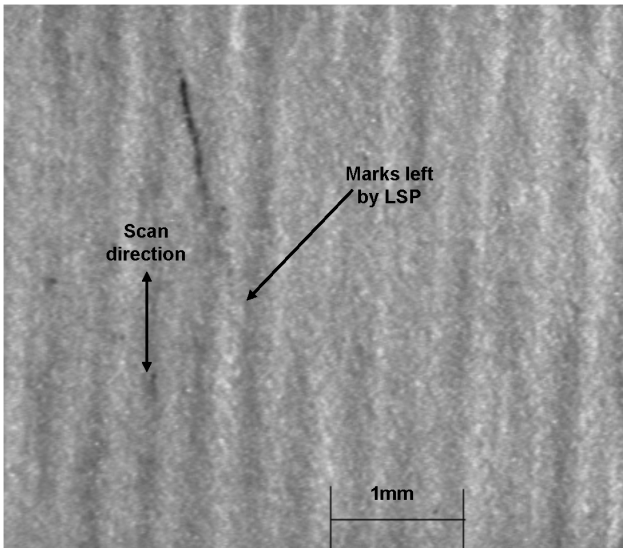

FIGURE 3. Photograph of the treated surface, note the marks left by the LSP.

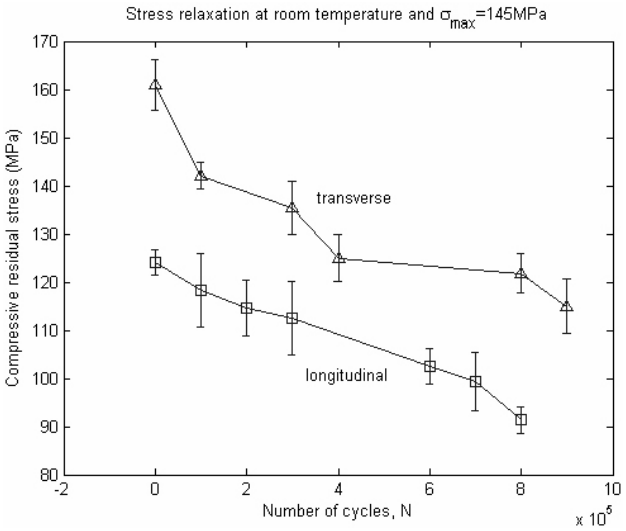

FIGURE 4. Stress relaxation at σ_{max}= 145MPa.

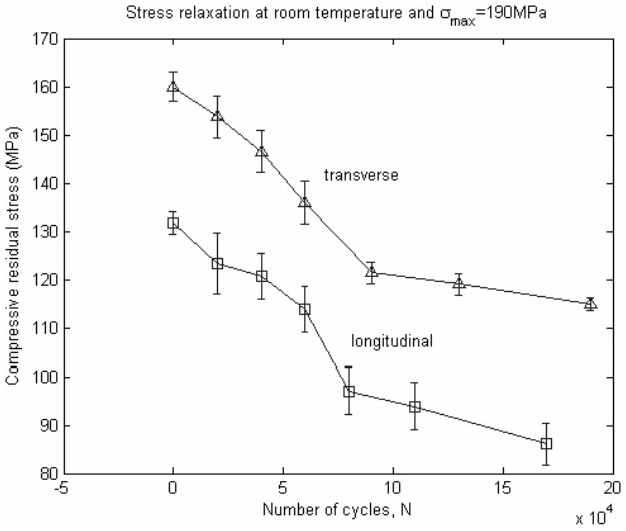

FIGURE 5. Stress relaxation at σ_{max}= 190MPa.

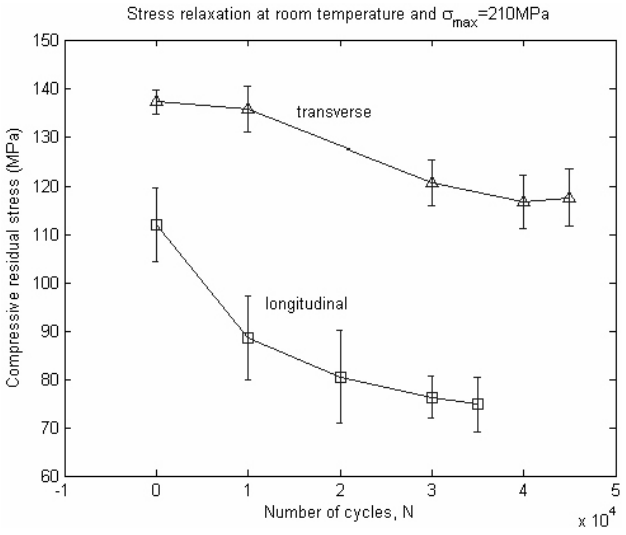

FIGURE 6. Stress relaxation at σ_{max}= 210MPa.

Residual stress measurement

The residual stresses were measured in an X-ray diffraction equipment Phillips X'Pert PRO operating in point focus geometry. The $\sin^2\Psi$ method was employed [16]. The system is equipped with a horizontal goniometer, a half circle cradle and an XYZ stage. A ceramic Cu long fine focus X-ray tube set to 45 kV and 40 mA is used for the X-ray generation. The incident beam PreFIX module is composed of a programmable divergence slit (PDS), 0.04 radians Sollers slits, antiscater slit $1/2$ degree and a 10 mm axial beam mask. The diffractometer radius is 240 mm [17]. In calculating the residual stress, lattice d-spacing vs. $\sin^2\Psi$ plots were used with 15 different Ψ angles. From the diffraction pattern, the peak used in the analysis was 2θ=139° corresponding to the plane $\{311\}$. The Young's modulus used in the residual stress calculation was E=59.7 GPa.

Relaxation tests

Once the specimens were treated with LSP, they were subjected to cyclic loading to evaluate the residual stress relaxation under different stress amplitudes and thermal conditions. Since the purpose of the experiments was to evaluate the stability of the initial residual stress field, the surface treatment was only applied at the beginning of the process; that is, no LSP treatment was made between cycles of loading. A number of cycles of loading were applied and then the residual stresses were measured. This process was repeated until the specimen failure. Following this procedure it was possible to obtain the curves of residual stress vs. number of cycles at room temperature (approximately 25°C) and at 150 and 170°C. Cyclic loading was applied on an MTS 810 testing machine at 40 Hz, using a sinusoidal wave form and for the high temperature tests a temperature controlled camera was used. Three maximum stresses (=σ_{max}) were considered at room temperature: 145, 190 y 210 MPa. For the high

temperature tests the maximum stress was only 145 MPa. In all the cases the stress ratio was

$$R = \sigma_{min}/\sigma_{max} = 0.1.$$

3. Results

Figures 4-6 show the curves of the compressive residual stress vs. the number of cycles for the experiments at room temperature under three external stress amplitudes. On each figure, one curve corresponds to the stress component along the force direction (longitudinal) and the other, to the component perpendicular to that direction (transverse). It is worth mentioning that the initial stress magnitude is different for each curve, this is due to the different material layer thickness removed during the initial grinding process on the specimen. The vertical lines indicate the standard deviation at each residual stress measurement.

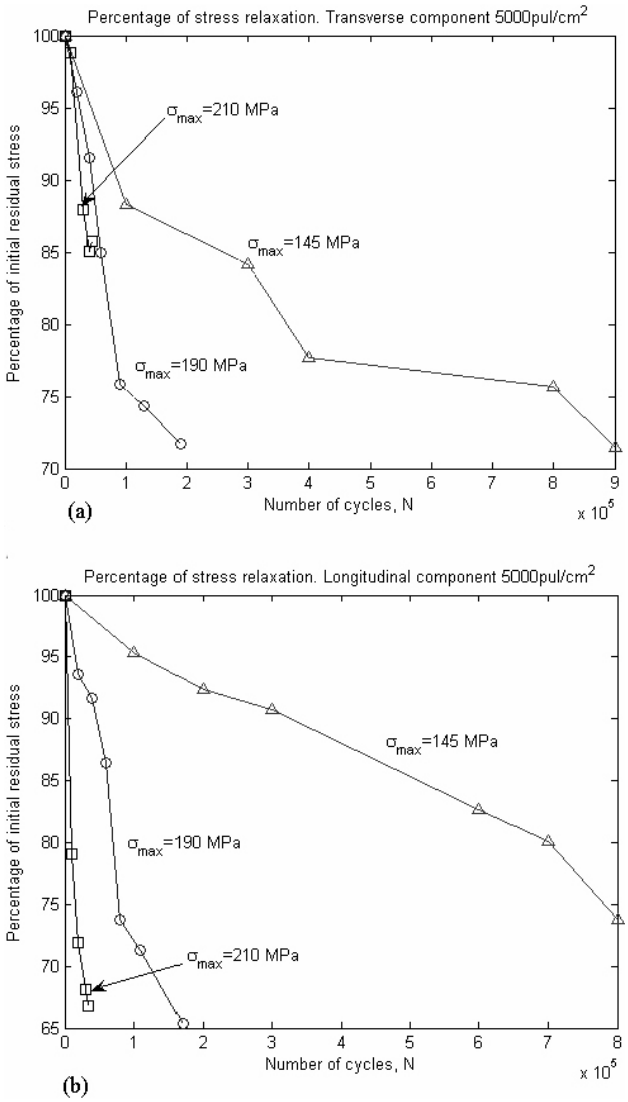

FIGURE 7. Percentage of stress relaxation with respect to the initial residual stress. (a) Transverse component, (b) Longitudinal component.

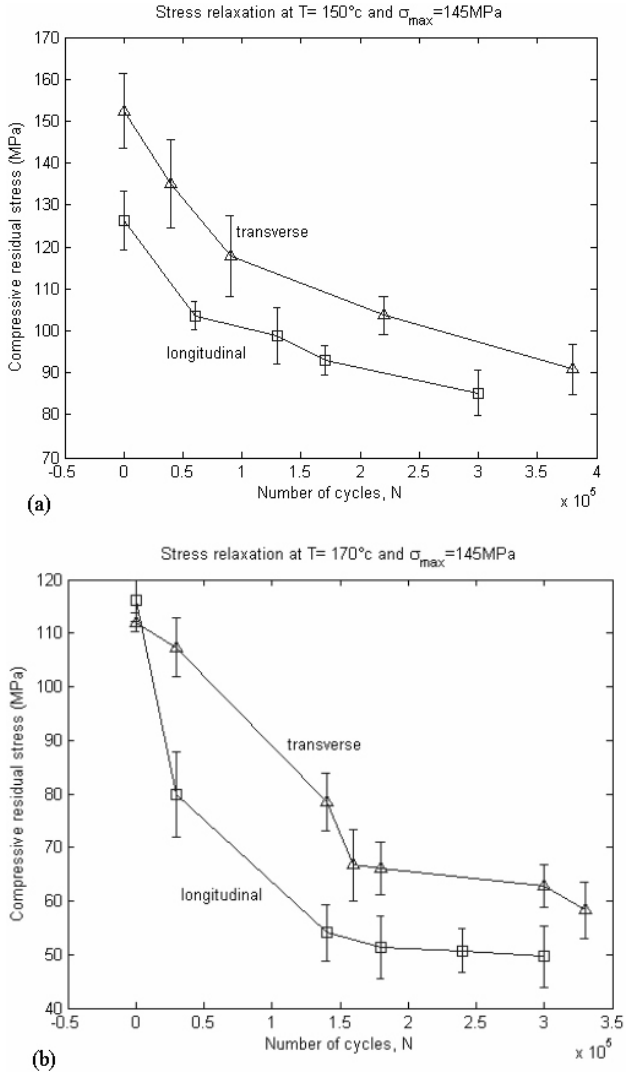

FIGURE 8. Stress relaxation at (a) T=150°C, (b) T=170°C.

From the residual stress distribution plots, Figs. 4-6, it is possible to observe that there is an effect of the pulse scan direction; *i.e.*, transverse compressive stress component being perpendicular to the scan direction is greater than the longitudinal component which is parallel to the scan direction. This effect has been explained in Ref. 15 and is due to the severe plastic distortion, with a well defined orientation, caused by the LSP scan process. In fact, superficial groves are observed along the scan direction as shown in Fig. 3.

From those results it is possible to make a comparison using the initial residual stress value as a reference. The *transverse* residual stress component, expressed as a percentage of the initial value is shown in Fig. 7a. Results for the three loading levels are shown. It is observed that as the maximum stress produced by the external load is increased, the relaxation rate is increased as well (recall that in all the cases R is constant). Similarly, the *longitudinal* residual stress components expressed as a percentage of the initial value are shown in Fig. 7b. It is noted here that applying cyclic loading with

a maximum stress of 145 MPa, we get the 74% of the initial residual stress at approximately 800×10^3 cycles, while applying a maximum stress of 190 MPa, we get 65% of the initial residual stress in 170×10^3 cycles and finally, applying a maximum stress of 210 MPa we get 66% of the initial value in only 35×10^3 cycles. This demonstrates that an increase in the cyclic stress amplitude increases the residual stress relaxation rate as well. Recall that the yield stress of the aluminum used in the experimental investigation and without LSP is 226 MPa.

Results similar to those at room temperature presented in Fig. 4 are shown in Figs. 8a and 8b but at temperatures of 150°C and 170°C, respectively. That is, in these experiments, the cyclic loading was applied with σ_{max}=145 MPa to the specimens inside a high temperature chamber. In this case, in addition to the effect of cyclic loading, the residual stress relaxation is due to the high temperature during the loading process. It is observed that the higher the temperature, the faster the stress relaxation process takes place. This fact is better appreciated in Fig. 9 where the compressive residual stress is expressed as a percentage of the initial residual stress. Fig. 9a shows the transverse stress component and Fig. 9b shows the longitudinal stress component. For example, in Fig. 9b we realize that at room temperature and with cyclic loading with maximum stress of 145MPa, we get the

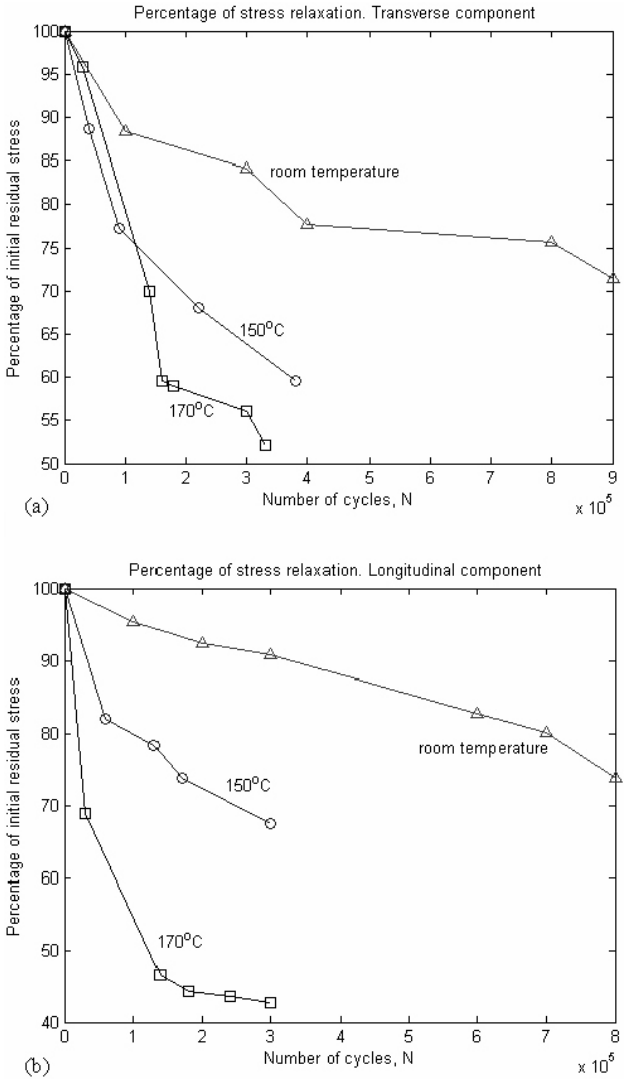

FIGURE 9. Evolution of the residual stresses expressed as a percentage of the initial value. (a) Transverse component, (b) Longitudinal component.

TABLE I. Stress relaxation rates for the different stress components and at different temperatures, values of m according to Eq. (1).

Temperature	transverse component	longitudinal component
Room	11.6	9.7
150°C	19.1	11.5
170°C	20.3	13.8

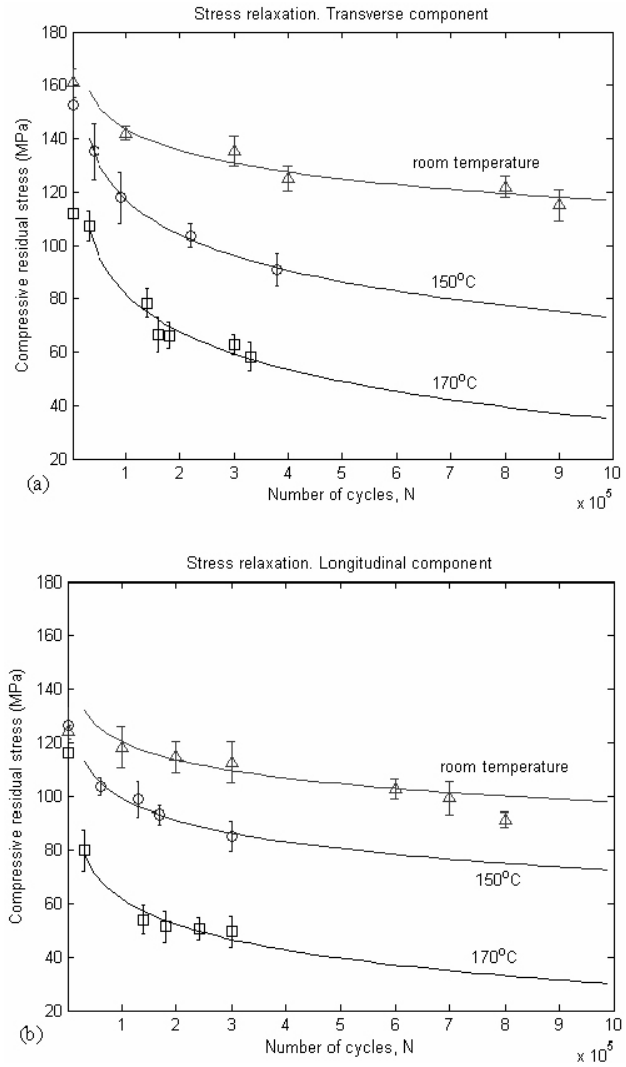

FIGURE 10. Stress relaxation due to cyclic loading (σ_{max}=145 MPa) applied at different temperatures. (a) Transverse component, (b) Longitudinal component.

74% of the initial residual stress at 800×10^3 cycles, while with the same loading conditions but at 150^{circ}C the residual stress reduces to the 67% of its initial value at 300×10^3 cycles and finally, at 170°C we get the 46% of the initial residual stress at only 140×10^3 cycles.

In order to quantify the stress relaxation rate, we may present the residual stress as a function of $\log(N)$, where N is the number of cycles. Fitting the experimental results to straight lines according to Eq. (1), we may find the slope m which may be associated with the stress relaxation rate. The values of m are presented in Table I. Fig. 10 shows the experimental results of the residual stress and the fitted lines given by Eq. (1). Note the high similarity between these results, this indicates that Eq. (1) is appropriate to describe the evolution of the residual stresses induced by LSP due to cyclic loading. For both stress components (transverse and longitudinal) we observe that increasing the temperature the value of m increases as well.

4. Summary

The stability of the residual stress field induced by Laser Shock Processing (LSP) during the application of thermal and mechanical energy has been analyzed on specimens of 6061-T6 aluminum alloy. The analysis shows that the higher the external cyclic loading amplitude, the higher the relaxation rate. It demonstrates as well, that increasing the environment temperature during the cyclic loading causes the stress relaxation to increase faster. The stress relaxation has been analyzed quantitatively through the logarithm creep law which describes the relaxation process due to cyclic loading applied at different temperatures.

1. C. Rubio-Gonzalez, *et al.*, *Mater. Sci. Eng.* **386** (2004) 291.
2. U. Sánchez-Santana, C. Rubio-González, G. Gomez-Rosas , J.L. Ocaña, and C. Molpeceres, **260** (2006) 847.
3. J.M. Yang Y.C. Her, N. Han, and A. Clauer, *Mater. Sci. Eng. A.* **298** (2001) 296.
4. Z Hong and Y. Chengye, *Mater. Sci. Eng. A.* **257** (1998) 322.
5. L.W. Tsay, M.C. Young, and C. Chen, *Corrosion Science* **45** (2003) 1985.
6. J.E. Rankin, M.R. Hill, and L.A. Hackel, *Mater. Sci. Eng. A.* **349** (2003) 279.
7. J.P. Chu, J.M. Rigsbee, G. Banas, and H.E. Elayed-Ali, *Mater. Sci. Eng. A.* **260** (1999) 260.
8. P. Peyre and R. Fabbro, **27** (1995) 1213.
9. K. Ding and L. Ye, *J. Mat. Proc. Tech.* **178** (2006) 162.
10. D. Lohe, O. Vohringer, Satibility of residual stresses, in: G. Totten, M. Howes, T. Inoue (Ed.) (Handbook of residual stress and deformation of steel, ASM International 2002).
11. H. Holtzafel, V. Schulze, O. Vohringer, and E. Macherauch, *Mater. Sci. Eng. A.* **248** (1998) 9.
12. W. Zhuang, G. R. Haldford, *Int. J. Fatigue* **23** (2001) S31.
13. I Nikitin, B Scholtes, H.J Maier, and I. Altenberger, *Scripta Materialia*, **50** (2004) 1345.
14. G. Gomez-Rosas, *et al.*, *Applied Surface Science* **252** (2005) 883.
15. C. Rubio-González, *et al.*, *Applied Surface Science* **525** (2006) 6201.
16. B.D. Cullity and R.S. Stock , *Elements of X-ray diffraction*, (Prentice-Hall, 2001).
17. X'Stress User Manual. (Phillips Analytical, 2002).